Effect of convection coefficient and thickness on optimal cure cycles for the manufacturing of wind turbine components using VARTM

Struzziero, G.; Teuwen, J. J.E.

DOI
10.1016/j.compositesa.2019.04.024

Publication date
2019

Document Version
Final published version

Published in
Composites Part A: Applied Science and Manufacturing

Citation (APA)
Struzziero, G., & Teuwen, J. J. E. (2019). Effect of convection coefficient and thickness on optimal cure cycles for the manufacturing of wind turbine components using VARTM. *Composites Part A: Applied Science and Manufacturing*, *123*, 25-36. https://doi.org/10.1016/j.compositesa.2019.04.024

Composites Part A 123 (2019) 25–36

Contents lists available at ScienceDirect

Composites Part A

journal homepage: www.elsevier.com/locate/compositesa

Effect of convection coefficient and thickness on optimal cure cycles for the manufacturing of wind turbine components using VARTM

G. Struzziero*, J.J.E. Teuwen

Faculty of Aerospace, Aerospace Manufacturing Technologies, Delft University of Technology, Delft 2628 CD, Netherlands

ARTICLE INFO

Keywords:
A. Thermosetting resin
B. Cure behaviour
C. Numerical analysis
E. Vacuum infusion

ABSTRACT

The paper deals with the influence of the convection coefficient and laminate thickness on multi-objective optimisation of the vacuum assisted resin transfer moulding cure stage for the manufacturing of wind turbine components. An epoxy resin system widely used in the wind turbine industry has been chemically characterised and the correspondent finite element implementation validated. The optimisation methodology developed links the finite element solution with a genetic algorithm and identifies a set of optimal cure cycles for a range of thicknesses (10–100 mm) able to minimise cure time (t_{cure}) and the maximum degree of cure gradient developed through thickness ($\Delta\alpha_{max}$) during the cure stage as a measure of quality of the product. The results highlight that, by adding convection coefficient as design parameter of the process, significant benefits could be obtained when insulation is applied at the vacuum bag side for all thicknesses.

1. Introduction

The manufacturing of structural parts for wind turbine blades poses serious challenges to the composite manufacturing industry due to the large thicknesses involved. The main girder, which is made by either carbon or glass fibre laminates, of a wind turbine is responsible to carry the bending loads and therefore its quality is crucial. Typical laminate thicknesses for these parts are about 50 mm whilst the root section that connects the blade with the hub goes up to 100 mm. The preferred manufacturing process in the wind industry is Vacuum Assisted Resin Transfer Moulding (VARTM). Given the dimension of the wind blades (up to 88 m in length to date), the single-mould nature of the VARTM process allows to contain the tooling cost. However, with the thicknesses at play, the curing stage of the Vacuum Assisted Resin Transfer Moulding (VARTM) manufacturing process of such parts becomes complex. The final mechanical performance of a composite laminate highly depends on a successful cure stage. Due to the low thermal conductivity in transverse direction of the composite laminates detrimental exothermic reaction and overshoot temperature are likely to happen as the thickness increases. The occurrence of violent temperature overshoots leads to significant differences in thermal history and therefore differences in degree of cure through thickness. This introduces different chemical shrinkage and thermal expansion which affects mechanical performance and life span of the part [1–3]. This phenomenon becomes even more pronounced when dealing with thick and ultra-thick components [4]. It is therefore crucial that the thermochemical properties of the part are accurately modelled to simulate the cure stage and that the cure profile selected is optimised to avoid or reduce the gradient in degree of cure through the thickness. Furthermore process time considerations need to be taken into account as they drive process costs. Identification of optimal cure cycles to address these objectives is needed as a trial and error approach or experience driven design choices may fail in producing reliable outcomes.

Researchers have been studying the optimisation of the cure stage by seeking optimal cure profiles to minimise either cost related objectives (i.e. process time) or quality related objectives (i.e. temperature overshoot, degree of cure/temperature gradients [1–3]). Attempts have also been made in the direction of addressing multiple objectives simultaneously. Optimal cure cycles for the minimisation of cure time have been addressed in literature for composite laminates made with epoxy resin and either glass or carbon fibre. The mechanical performance of the parts was ensured by setting quality control constraints such as maximum overshoot temperature allowed or cure uniformity through thickness. The thicknesses were in the range of 10–50 mm [5–13]. The optimisation problem of maximising performance has been investigated either by maximising final degree of cure of the part or by minimising residual stresses and distortion for part thicknesses in the range of 4–60 mm. Cure time constraints were applied to ensure reasonable duration of the process [14–22]. In the attempt to address both cost related and quality related objectives, researchers have been

* Corresponding author.
E-mail address: G.Struzziero@tudelft.nl (G. Struzziero).

https://doi.org/10.1016/j.compositesa.2019.04.024
Received 28 February 2019; Received in revised form 11 April 2019; Accepted 20 April 2019

designing single weighted fitness functions to be minimised by finding optimal cure profiles. Thicknesses were in the range of 5–25 mm [23–28]. A multi-objective optimisation problem to minimise cure time and maximum overshoot temperature by finding optimal cure cycles was carried out for 24 mm and 60 mm components. In addition to this, it was shown that variation in convection coefficient could significantly affect the outcome of the cure process [4]. A stochastic model of the cure process using surrogate model representation had been undertaken; the model had been linked with a GA for multi-objective problems. Optimal cure cycles were identified and reductions of about 40% were achieved in both temperature overshoot and cure time compared to standard cure profiles. Furthermore the reduction was accompanied by 20% variability reduction in both objectives [29]. However, little attention has been devoted to the influence of convection coefficient and to thicknesses reaching up to 100 mm on the VARTM process and on its optimal cure cycle solutions.

The aim of the paper is to look into the effect of convection conditions on optimal cure cycles to minimise cure time (t_{cure}) and maximum degree of cure gradient through thickness ($\Delta\alpha_{max}$) experienced by the part during the curing process at each time step. To highlight the effect of the convection coefficient on the optimisation problem, three different thicknesses are considered. Solutions obtained when a constant natural convection boundary condition at the vacuum bag side (13.6 W/m^2 °C) is applied and when an optimisable convection coefficient between insulation (1 W/m^2 °C) and improved heat exchange with environment (20 W/m^2 °C) is addressed, are compared. The effect of thickness on the outcomes of the optimisations will be discussed for both the natural convection coefficient and the optimisable convection coefficient scenario. Also the effect of different thicknesses (10 mm, 50 mm and 100 mm) on the optimisation problem and on the achievable trade-offs between the objectives will be addressed in detail in the paper. The study is limited to the manufacturing of glass fibre/epoxy composite laminate via VARTM process which is a single-mould process occurring on a hot tool closed with a flexible vacuum bag at the top end, mimicking the industrial application. An epoxy resin system widely used in the wind industry has been chemically characterised. The optimisation methodology linking multi-objective Genetic Algorithm (GA) with Finite Element (FE) model is adapted and implemented [4]. A solution of the cure stage of a VARTM process is carried out. Optimal sets of cure profiles and convection coefficient capable to minimise t_{cure} and $\Delta\alpha_{max}$ are identified and studied. The Pareto fronts obtained are also compared with the outcomes achieved when Manufacturer Recommended Cure Cycle (MRCC) is applied to the three different thicknesses.

2. Material sub-models

The heat transfer equation to solve to tackle the problem is the following:

$$\rho_c c_{pc} \frac{\partial T}{\partial t} = \nabla(k_c \nabla T) + Q \tag{1}$$

Here ρ_c, c_{pc} and k_c represents the density, heat capacity and thermal conductivity of the composite whilst T is the temperature. The term Q represents the heat generated by a source which in our case is given by the exothermic reaction of the resin and can be written as follows:

$$Q = \rho_r v_r H_r \frac{d\alpha}{dt} \tag{2}$$

where ρ_r is the density of the resin, v_r the resin volume fraction, H_r the total heat generated by the resin and $\frac{d\alpha}{dt}$ the reaction rate of the resin. In order to solve the equation a number of constitutive material models need to be available namely: cure kinetics, specific heat and thermal conductivity of the resin plus the specific heat and thermal conductivity values of the fibre to compute the specific heat and thermal conductivity of the composite.

2.1. Chemical characterisation

The materials considered in this study are a non-crimp biaxial E-glass fibres fabric and the two component Airstone™ 780E epoxy resin and 785H Hardener system [30] used in wind turbine blade manufacturing. The cure kinetics characterisation campaign of the resin system has been carried out. A Perkin Elmer® Differential Scanning Calorimetry (DSC) has been used for the characterisation campaign. Four isothermal tests at 50, 70, 90 and 110 °C and one dynamic test at 1 °C/min have been carried out.

The development of the glass transition temperature of the system has been also characterised. The samples were heated in the DSC at 1 °C/min up to increasing final temperature and quickly cooled down to stop the cure. This was performed in order to produce different levels of partially cured samples. Subsequently the samples were heated at 10 °C/min to identify the glass transition temperature in the heat flow signal. Three repeated tests per final temperature were run. The degree of cure reached by each sample was extrapolated from the 1 °C/min dynamic experiment.

To validate the degree of cure prediction of the cure kinetics some additional validation tests were required. Pure resin samples with different degrees of cure were manufactured using mould of rectangular shape made of two aluminium plates with a slit in between. Rectangular shape samples with dimensions of 170 × 110 × 2.5 mm were manufactured. The freshly mixed resin was poured in the slit between the two aluminium plates, a thermocouple was located in the epoxy resin and after that the mould was placed in the oven to cure. Four different cure profiles have been used to manufacture samples with different degrees of cure namely 45 min at 70 °C, 95 min at 70 °C, 255 min at 70 °C and 135 min at 110 °C. After that, small pieces for DSC analysis were scraped from the original samples. A DSC run at 10 °C/min was subsequently performed to identify the glass transition temperature of each manufactured plate. The effective thermal history that the resin underwent was measured by the thermocouple and fed to the cure kinetics model which provides the degree of cure of the sample.

2.2. Thermal properties

The specific heat capacity of the composite is obtained by computing the specific heat of E-glass fibres and epoxy resin. Thermal properties of the resin under study have been measured for the fully cured system at room temperature. The resin shows a thermal conductivity of 0.27 W/m °C and a specific heat of about 1200 J/Kg °C [31]. Among the few available data for thermal conductivity [32] the RTM6 epoxy resin match well these values for the fully cured samples therefore its constitutive models have been implemented. Validation of the heat transfer will prove the goodness of the assumption. The specific heat capacity of fibre, c_{pf}, and resin, c_{pr}, are represented as follows [4,33]:

$$c_{pf} = A_{f_{cp}} T + B_{f_{cp}} \tag{3}$$

$$c_{pr} = A_{rc_p} T + B_{rc_p} + \frac{\Delta_{rc_p}}{1 + e^{C_{rc_p}(T - T_g - \sigma)}} \tag{4}$$

where $A_{f_{cp}}$ and $B_{f_{cp}}$ are fitting parameters of the linear dependence of fibre specific heat capacity on temperature. The specific heat model of the resin presents step behaviour when transition occurs. A_{rc_p} and B_{rc_p} are constants expressing the linear dependence of the specific heat capacity of the uncured epoxy on temperature and Δ_{rc_p}, C_{rc_p} and σ are the strength, width and temperature shift respectively of the step transition occurring at resin vitrification. The specific heat of the composite is then computed applying the rule of mixture formula:

$$c_p = w_f c_{pf} + (1 - w_f) c_{pr} \tag{5}$$

here w_f stands for the weight fibre fraction. Table 1 reports the fitting parameters for the specific heat material model for both the resin and E-

Table 1
Parameter values for material property sub-model of the coupled thermo-chemical simulation [4,33].

Parameters	Values	Units
A_{fc_p}	0.0014	J g^{-1} °C^{-2}
B_{fc_p}	0.841	J g^{-1} °C^{-1}
A_{rc_p}	0.0025	J g^{-1} °C^{-2}
B_{rc_p}	1.80	J g^{-1} °C^{-1}
Δ_{rc_p}	−0.25	J g^{-1} °C^{-1}
C_{rc_p}	1.10	°C^{-1}
σ	16.5	°C
a_{Kr}	0.0008	W m^{-1} °C^{-2}
b_{Kr}	−0.0011	W m^{-1} °C^{-2}
c_{Kr}	−0.0002	W m^{-1} °C^{-2}
d_{Kr}	−0.0937	W m^{-1} °C^{-1}
e_{Kr}	0.22	W m^{-1}° C^{-1}
f_{Kr}	0.12	W m^{-1}° C^{-1}
ρ_f	2580	kg m^{-3}
ρ_r	1105	kg m^{-3}

glass fibre [4,33].

The thermal conductivity of the composite is computed by accounting the contributions from both resin and glass fibres. The longitudinal component K_{11} and transverse components K_{22}, K_{33} can be calculated as follows [34]:

$$K_{11} = v_f K_{lf} + (1 - v_f) K_r \tag{6}$$

$$K_{22} = K_{33} = v_f K_r \left(\frac{K_{tf}}{K_r} - 1\right) + K_r \left(\frac{1}{2} - \frac{K_{tf}}{2K_r}\right) + K_r \left(\frac{K_{tf}}{K_r} - 1\right) \sqrt{v_f^2 - v_f + \frac{\left(\frac{K_{tf}}{K_r} + 1\right)^2}{\left(\frac{2K_{tf}}{K_r} - 2\right)^2}} \tag{7}$$

where v_f is the fibre volume fraction, K_{lf} and K_{tf} are the longitudinal and transverse thermal conductivities of the fibres which in the case of glass fibres coincide and is equal to 1.03 W/m °C. As for the thermal conductivity of the resin, K_r, values from literature have been used [4].

$$K_r = a_{Kr} T\alpha^2 + b_{Kr} T\alpha + c_{Kr} T + d_{Kr} \alpha^2 + e_{Kr} \alpha + f_{Kr} \tag{8}$$

Here a_{Kr}, b_{Kr}, c_{Kr}, d_{Kr}, e_{Kr} and f_{Kr} are coefficients of the polynomial function describing the resin thermal conductivity dependence on temperature and degree of cure. The fitting parameters of the thermal conductivity sub-models are reported in Table 1 [4].

3. Cure simulation

The thermo-chemical problem occurring during the cure of the composite part is modelled and solved using the Finite Element solver Marc.Mentat® [35]. The elements used for the simulation are three-dimensional isoparametric 8-nodes brick composite for heat transfer analysis (Marc® element type 175) [36]. Material properties and boundary conditions are implemented using user subroutines [37]. With regard to the FEA models used for the optimisation procedure, since VARTM process is used by the wind turbine industry natural air convection boundary condition at the vacuum bag side is applied using UFILM user subroutine. The ambient temperature considered for the natural convection is 25 °C whilst the convection coefficient is equal to 13.6 W/m^2 °C in the case where the convection coefficient is kept constant [38]. Since curing during the manufacturing of wind turbine blades occur on a hot tool, time dependent fixed temperature boundary condition is applied at the nodes in contact with the mould following the thermal profile set by the optimisation with FORCDT user subroutine. Initial temperature condition equal to ambient temperature is applied to all the nodes in the model. The cure kinetics were implemented using the UCURE user subroutine whilst thermal properties such as specific heat and thermal conductivity were implemented using USPCHT and ANKOND user subroutines. Fig. 1 depicts a schematic of the model boundary condition application. Although the models are implemented in a 3D analysis the temperature evolution is as a matter of fact one dimensional. This is achieved by using a single element for both in plane directions which alongside the implied zero heat flux boundary condition on the corresponding boundaries results in infinite length and width. In the through-thickness direction the model comprises 16 elements and 68 nodes. A mesh convergence analysis has been performed for the 100 mm thick component. The number of elements was kept the same also for the thinner parts as the computational time for one run was in the order of minutes.

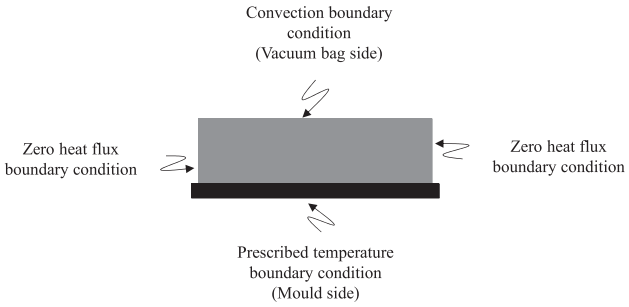

Fig. 1. Schematic of model boundary conditions.

4. Multi-objective optimisation methodology

The multi-objective optimisation problem has been set in order to find optimal cure cycles and convection condition that minimise t_{cure} (cost related objective) and $\Delta\alpha_{max}$ (quality related objective). The MRCC for the resin system under study imposes a one dwell profile at 70 °C. The optimal cure profiles have been sought among two dwells cycles [3]. Therefore four parameters have been identified for parameterisation, namely: temperature of first and second dwell (T_1, T_2), duration of the first dwell (Δt_1) and ramp rate (r). Furthermore the convection coefficient (h) has been added as parameter of the optimisation. Fig. 2 reports the general shape of the MRCC and the shape of the proposed parameterisation of the two dwell profile. A GA capable to deal with multi-objective optimisation problems has been adapted and tuned for the problem under study. The GA adopted has been tested against standard benchmarks problem and its reliability and results reproducibility assessed [4]. Table 2 reports the range investigated in the optimisation runs for each parameter. Regarding T_1, a temperature of 30 °C has been chosen as lower limit since it would be not feasible curing at temperature lower than ambient. The upper limit is set at 70 °C as this is the MRCC temperature. The upper limit of T_2 is set at 105 °C due to technological limitation of the moulds. The first dwell duration range has been selected in order to allow the GA to select one dwell scenarios in the case of t_{cure} shorter than Δt_1. Ramp rate range has been decided according to technological limitation of the mould used in industry. As for the convection coefficient, according to [36], the standard natural convection coefficient is equal to 13.6 W/m^2 °C therefore the range has been chosen in order to allow scenarios where insulation is applied (h < 13.6 W/m^2 °C) and scenarios where improved heat exchange with the environment is applied (h > 13.6 W/m^2 °C). The t_{cure} is defined as the time at which the minimum degree of cure reached in the model is 93% therefore the duration of the second dwell is not a parameter of the optimisation. The 93% degree of cure threshold is chosen as this is the degree of cure reached by the epoxy resin with an isothermal DSC run at the cure temperature of 70 °C.

A total of three test cases have been taken into account. The components are flat panels with different thicknesses. The thicknesses addressed are 10 mm for the thin case, 50 mm for the thick case

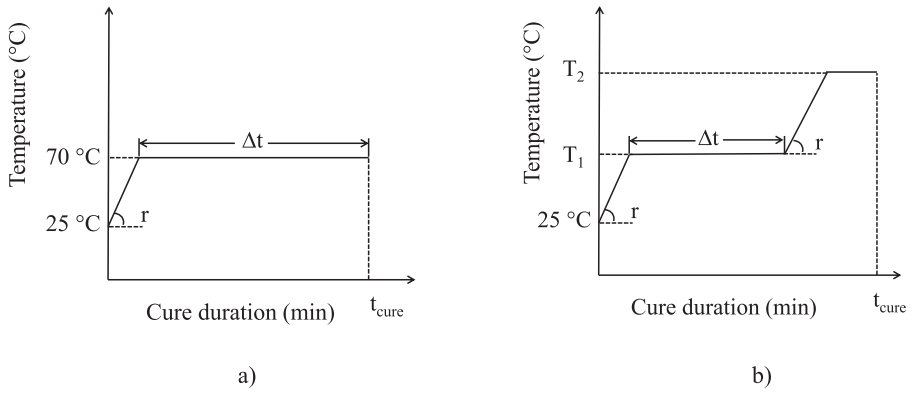

Fig. 2. (a) Parameterised MRCC. (b) Parameterised two dwell cure cycle.

Table 2
Design parameter ranges.

Parameters	Ranges	Units
T_1	30–70	°C
T_2	70–105	°C
Δt	2–240	min
r	0.1–4.0	°C min^{-1}
h	1–20	W m^{-2} °C^{-1}

Table 3
Optimisation parameters.

GA input	Flat panel	
	10 mm	50/100 mm
Max number of generations	20	20
Individuals per population	50	100
Individuals per reproduction	40	80
Elite individuals	4	8
Size of Pareto set	30	40
Mutation probability	0.005	0.005
Cross-over probability	0.5	0.5

resembling the girder of the wind blade and 100 mm which is typical thickness of root insert sections. Initial and boundary conditions applied to the models are as described in Section 3. The optimisation methodology uses an interface built in C++ to link the GA optimiser and the FE models built in Marc.Mentat. Fig. 3 illustrates the function of the interface. The GA generates a new set of four or five parameters at each iteration depending on whether the convection coefficient is considered. The interface creates a copy of the Marc.Mentat input file by copying line by line the old input file and updating at the correct location the new file inserting the new parameters generated. After that a command to execute the FE simulation with the modified input file is run. During the simulation run the objective of interest are made available by user subroutines [37]. The UPSTNO user subroutine read the temperature and degree of cure at each increment of the simulation and the $\Delta\alpha_{max}$ for the corresponding increment is stored into a variable. Once the minimum degree of cure threshold is reached the UEDINC user subroutine withdraw the corresponding t_{cure} and store the value into a variable. At the end of the run the interface writes the values of t_{cure} and $\Delta\alpha_{max}$ in two text files. The interface opens the text files, reads the values and sends them to the GA. At this point a new iteration starts. Table 3 reports the GA optimisation parameters used for the three cases. The number of individuals per population, of individuals used per reproduction and elite individuals has been doubled for the thick and ultra-thick cases with respect to the thin case. The non-linearity of the cure process increases with thickness making the landscape of the problem riddled with more local minima where the GA can get trapped [4]. Increasing the size of the initial population helps the GA to not get trapped in local minima.

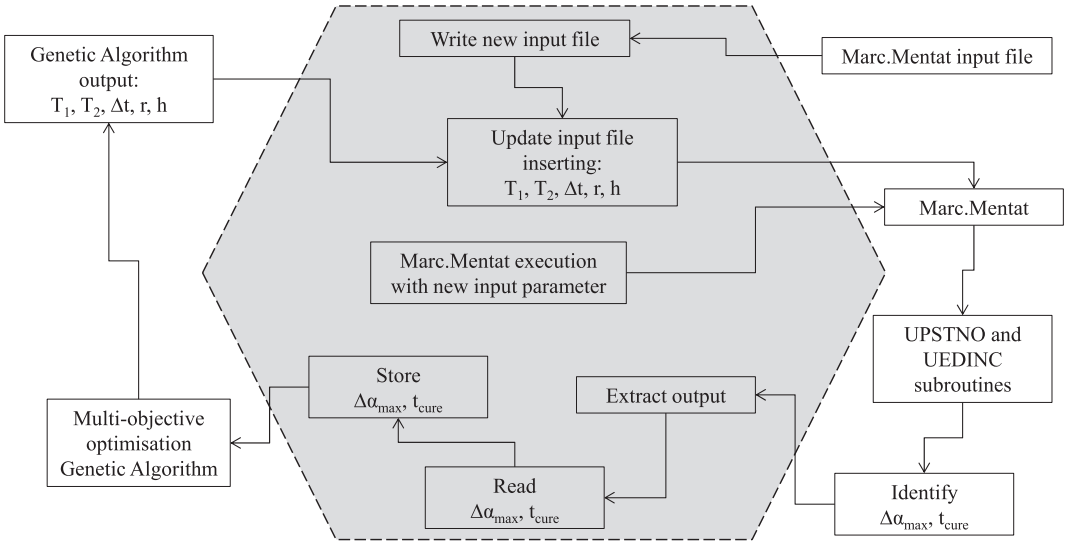

Fig. 3. GA and FE communication interface.

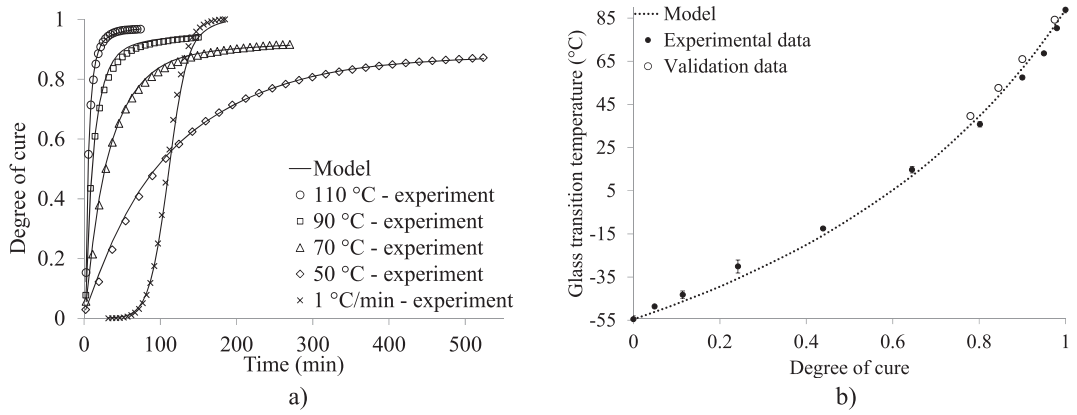

Fig. 4. Airstone™ 780E/785H system model fitting (a) Cure kinetics. (b) Di Benedetto equation with validation data points.

5. Results and discussion

5.1. Resin cure kinetics and Di Benedetto equation

The experimental data have been fitted with the following kinetics model proposed by Khoun et al. [39]:

$$\frac{d\alpha}{dt} = \frac{Ae^{\left(\frac{-E}{RT}\right)}}{1 + e^{C(\alpha-\alpha_c-\alpha_T T)}}(1-\alpha)^n\alpha^m \tag{9}$$

where α is the degree of cure, α_c, α_T, are coefficients controlling the transition of the kinetics from chemical to diffusion control, m, n are reaction orders for the n-th order and autocatalytic terms, A is a pre-exponential Arrhenius factor, E is the activation energy of the Arrhenius functions, T is the absolute temperature, R is the universal gas constant. Fig. 4(a) reports the fitting of the experimental data with the proposed models whilst Table 4 reports the fitting parameters.

The glass transition temperature model to fit the experimental data follows the Di Benedetto equation [40]:

$$T_g = T_{go} + \frac{(T_{g\infty} - T_{go})\lambda\alpha}{1-(1-\lambda)\alpha} \tag{10}$$

here $T_{g\infty}$ and T_{go} are the glass transition temperatures of the fully cured and uncured material respectively and λ is a fitting parameter governing the convexity of the dependence. Fig. 4(b) illustrates the quality of the fitting together with the validation data points and Table 4 reports the fitting parameters of the cure kinetics and glass transition temperature development models.

5.2. Cure model experimental validation

In order to validate the cure kinetics and the through-thickness heat transfer model developed, two laminates have been manufactured. The laminates were manufactured using non-crimp biaxial E-glass fibre with 812 g/m^2 and the NEG 2001/2002 sizing and the Airstone™ epoxy system characterised in this study. The lay-up was $[45/-45]_{4s}$ and volume fibre fraction 54%. The thickness of the manufactured laminates was 31.5 mm. The two laminates were manufactured following two different cure cycles. For symmetry reasons, an aluminium plate was placed at the top of the laminate. The first cure cycle prescribes a ramp at 0.83 °C/min up to 50 °C, 50 min dwell at 50 °C, ramp at 0.83 °C/min up to 100 °C, 400 min dwell at 100 °C, the second cycle was the MRCC which dictates a ramp at 0.33 °C/min up to 70 °C and an isothermal dwell at 70 °C for 240 min [30]. The aim of the tests is to monitor the temperature evolution through the thickness and compare the data from the experiment with the cure simulation prediction. One thermocouple was placed at 15 mm and one at 1 mm through thickness. The laminate infusion occurs at room temperature. The infusion time for the two laminates was in the range of 101–104 min. To validate the heat transfer model and the cure kinetics through the thickness of the laminate a convection boundary condition has been applied at the top and bottom of the two aluminium plates with a sink temperature following the cure profile and a convection coefficient of 13.6 W/m^2 °C [38] since the curing occurred inside the oven. The cure model with the aforementioned boundary conditions has been run and the thermal history predicted by the model for the nodes at 15 mm and at 1 mm through thickness have been compared with the ones detected by the thermocouples placed at the same locations during the experiment. Fig. 5 shows the comparison between the predicted and measured temperature at 1 mm and 15 mm thickness of the laminate. The agreement between model prediction and measurements is highly satisfactory. The accuracy with which the FE model predicts the temperature evolution through thickness guarantees that the thermal properties adopted in this study are adequate for the resin system studied and that the exothermic reaction described by the cure kinetics is accurate.

Table 4
Fitting parameters values for the cure kinetics and glass transition temperature material sub-models of Airstone™ 780E/785H system.

Parameters	Values	Units
A	681,085	s^{-1}
E	59,291	J mol^{-1}
n	1.67	
m	0.12	
C	47.7	
α_c	0.77	
α_T	0.0016	K^{-1}
H_{tot}	434	J g^{-1}
T_{go}	−55	°C
$T_{g\infty}$	89	°C
λ	0.476	

5.3. Multi-objective optimisation results

Figs. 6–8 report the results of the multi objective optimisation for the thin (10 mm), thick (50 mm) and ultra-thick (100 mm) case respectively. In all cases, the optimisation converges to a Pareto front highlighting the existence of optimal trade-offs between the objectives selected. The optimisation methodology is able to identify and quantify the efficiency solutions existing within the landscape of the problem. The L-shape of the Pareto fronts points out the competitive nature of the cost and quality related objectives, enforcing the necessity of a multi-objective analysis. It also suggests that a division of the objective space in two regions exist. One in which cure time is prioritised over the $\Delta\alpha_{max}$ and significant improvements can be obtained in the $\Delta\alpha_{max}$ with small changes in cure time (vertical part) and one where high

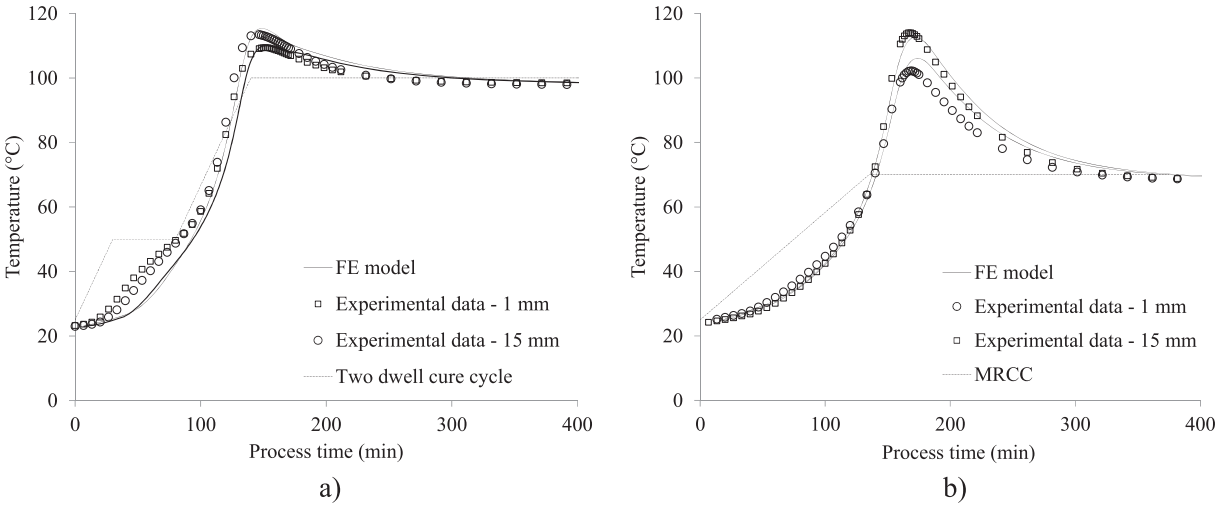

Fig. 5. Temperature evolution comparison between experimental data and FE prediction at 1 mm and 15 mm of the laminate for two different cure cycles. (a) Two dwell cure cycle. (b) MRCC.

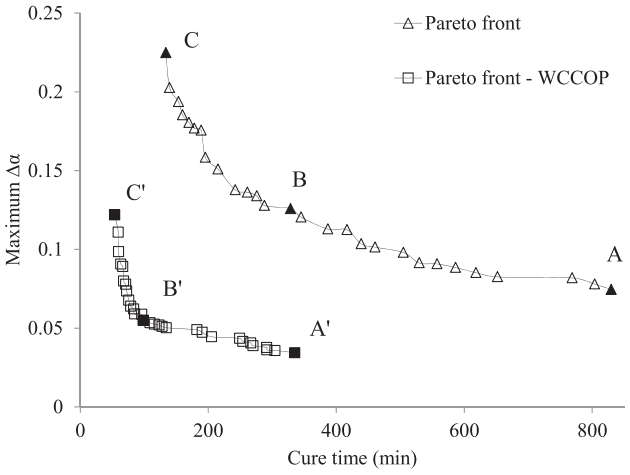

Fig. 6. Optimisation results for the 10 mm flat panel: Pareto fronts comparison With Convection Coefficient as Optimisation Parameter (WCCOP) (i.e. A′, B′, C′) and without (i.e. A, B, C).

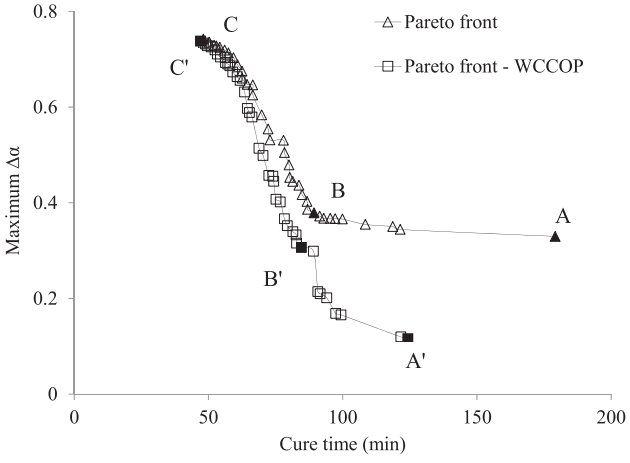

Fig. 7. Optimisation results for the 50 mm flat panel: Pareto fronts comparison With Convection Coefficient as Optimisation Parameter (WCCOP) (i.e. A′, B′, C′) and without (i.e. A, B, C).

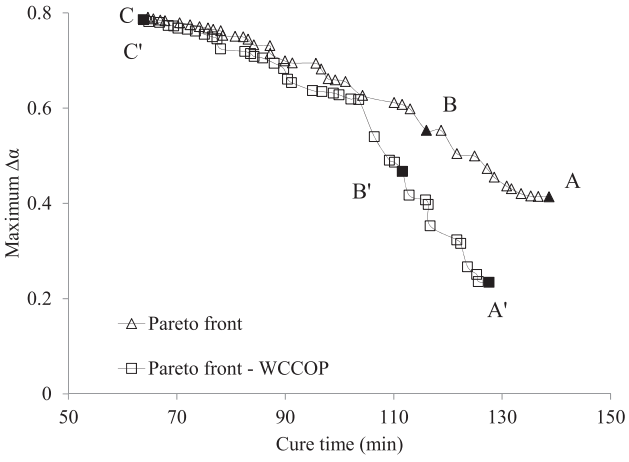

Fig. 8. Optimisation results for the 100 mm flat panel: Pareto fronts comparison With Convection Coefficient as Optimisation Parameter (WCCOP) (i.e. A′, B′, C′) and without (i.e. A, B, C).

importance is given to the $\Delta\alpha_{max}$ and significant improvements in cure time can be achieved with little change in the $\Delta\alpha_{max}$ (horizontal part). The maximum temperature reached by the solutions in the final Pareto fronts never exceeds 200 °C. The degradation temperature for the current system is 330 °C, therefore each solution belonging to the final Pareto fronts can be accepted since the maximum temperature stays well below the degradation temperature of the resin. In the following sections the results of the 10, 50, and 100 mm optimisations will be discussed in more detail. Afterwards, the effect of adding the convection coefficient to the optimisation and the effect of thickness of the laminates will be described. Finally, a comparison of the optimisation results with the results when the manufacturing recommended cure cycle is applied will be described.

5.3.1. Flat panel 10 mm results

The optimisation results for the 10 mm flat panel are reported in Fig. 6. For this case convergence of the Pareto is achieved after 15 generations. A comparison between the Pareto obtained using only the cure profile parameters and with the addition of convection coefficient as optimisation parameter (WCCOP in Fig. 6) is shown. The introduction of the convection coefficient as design parameter brings significant benefits, shifting the Pareto towards shorter curing time and lower degree of cure gradients, achieving approximately 50% reduction in

Table 5
Design parameters for the 10, 50 and 100 mm flat panel individuals.

Zone		Design parameters						
		T_1 (°C)	T_2 (°C)	Δt (min)	r (°C min^{-1})	h (W m^{-2} °C^{-1})	$\Delta\alpha$	t_{cure} (min)
10 mm flat panel								
Pareto front without convection coefficient as optimisation parameter								
A	Conservative	43.3	104.3	210	0.13	13.6	0.07	805
B	Transitional	57.8	103.7	140	0.87	13.6	0.12	330
C	Non-conservative	68.2	104.8	2	3.4	13.6	0.22	135
Pareto front with convection coefficient as optimisation parameter								
A′	Conservative	54.3	102.3	210	0.8	1	0.03	335
B′	Transitional	66.7	104.5	5	1.4	1	0.06	100
C′	Non-conservative	66.7	104.5	2	3.8	1	0.12	55
50 mm flat panel								
Pareto front without convection coefficient as optimisation parameter								
A	Conservative	51.8	103.7	50	2.3	13.6	0.33	180
B	Transitional	61.3	105.1	46	3.6	13.6	0.38	90
C	Non-conservative	67.8	105.1	4	3.5	13.6	0.73	50
Pareto front with convection coefficient as optimisation parameter								
A′	Conservative	41.7	101.5	77	4	1	0.11	124
B′	Transitional	61.3	104.3	41	3.7	1.6	0.31	85
C′	Non-conservative	64.1	104.3	2	3.9	1	0.73	48
100 mm flat panel								
Pareto front without convection coefficient as optimisation parameter								
A	Conservative	30.4	100.7	90	3.4	13.6	0.41	140
B	Transitional	39.8	104.3	80	3.6	13.6	0.55	115
C	Non-conservative	52.5	103.2	2	3.9	13.6	0.79	65
Pareto front with convection coefficient as optimisation parameter								
A′	Conservative	30.4	104.5	80	3.1	1	0.23	125
B′	Transitional	36.4	104.5	65	3.4	1	0.47	110
C′	Non-conservative	57.5	102.3	2	3.4	3.4	0.78	60

$\Delta\alpha_{max}$ and 75% reduction in cure time. All the individuals in the final Pareto present convection coefficients close to 1 W/m^2 °C meaning that insulation at the vacuum bag side brings benefits in both objectives. From Fig. 6 it is possible to identify three main zones in both graphs around which individuals tend to cluster. These zones translate into specific design choices. A quality conservative zone that allows longer process time to ensure small degree of cure differences through thickness, a quality non-conservative zone that allows higher degree of cure gradients during the process to favour process time and a transitional zone in which mixed behaviour can be identified. Table 5 reports the design parameters of candidate individuals (corresponding to A, B, C, A′, B′, C′ in Fig. 6) picked out of each zone for the 10 mm flat panel case. All the individuals show a high second dwell between 102 and 105 °C. Specifically when only the four cure cycle parameters are optimised (i.e. without optimising the convection coefficient), conservative zone individuals (i.e. A) are characterised by a low first dwell temperature (i.e. 43 °C), long first dwell duration (i.e. 208 min) and very mild ramp rate (i.e. 0.13). The design parameters for this zone point toward mild development of the reaction switching to the higher second dwell once the chemical potential of the resin has been exploited and an increase in temperature will not trigger violent exothermic reaction. As a result the final part has the lowest $\Delta\alpha_{max}$ (i.e. 0.07) but a long t_{cure} (i.e. 803 min). Moving toward the other two zones (i.e. B, C) the trend shown is to seek faster t_{cure}. This is achieved by increasing the temperature of first dwell (i.e. 57.8 °C for the transitional and 68.2 °C for the non-conservative zone), decreasing the duration of first dwell (i.e. 138 min for the transitional and 2 min for the non-conservative zone) and by increasing the ramp rate (i.e. 0.87 °C/min for the transitional and 3.4 °C/min for the non-conservative). This results in shorter t_{cure} but higher $\Delta\alpha_{max}$ during the process (i.e. 0.12 for the transitional and 0.22 for the non-conservative zone) and therefore progressively lower quality of the part. When the convection coefficient is added as optimisation parameter, optimal individuals (i.e. A′, B′, C′) show a value close to 1 W/m^2 °C meaning that insulation on the vacuum bag side of the process is beneficial in terms of both objectives. The introduction of insulation at the top allows more aggressive design parameter choices (i.e. higher ramp rate and first dwell temperature and shorter first dwell duration) compared to the case without it and resulting in significant improvements in both objectives.

5.3.2. Flat panel 50 mm results

Fig. 7 reports the optimisation results for the flat panel 50 mm cases. Convergence is reached after nine generations. Observing the design parameters that led to the Pareto front it is possible to identify three categories of individuals in the Pareto behaving similarly. Candidate individuals (i.e. A, B, C, A′, B′, C′) are picked out the Pareto front and highlighted in Fig. 7. Table 5 reports the details of these individuals. All the individuals present a high second dwell in the range of 101–105 °C. When convection coefficient is not used as optimisation parameter the conservative individuals (i.e. A) show a first dwell temperature of about 52 °C, with duration of about 50 min and 2.3 °C/min ramp rate. The cure ends after 180 min with the lowest $\Delta\alpha_{max}$. As the thickness increases it becomes more challenging to keep the cure time long and therefore develop mild reaction. An increase in first dwell temperature together with a decrease in first dwell duration marks the passage from conservative zone towards transitional and non-conservative zones (i.e. B, C respectively). These individuals present first dwell temperature higher than 60 °C, shorter first dwell duration (46 min for individual B and 4 min for individual C) and a quick ramp up to the second dwell (3.5 °C/min). This results in shorter t_{cure} (90 and 50 min for individual B and C respectively) but higher $\Delta\alpha_{max}$, 0.38 and 0.73 for individual B and C respectively. In this case, the introduction of convection as parameter brings benefits (up to 50% reduction in $\Delta\alpha_{max}$) for the individuals in the conservative zone whereas the benefits are negligible in the non-

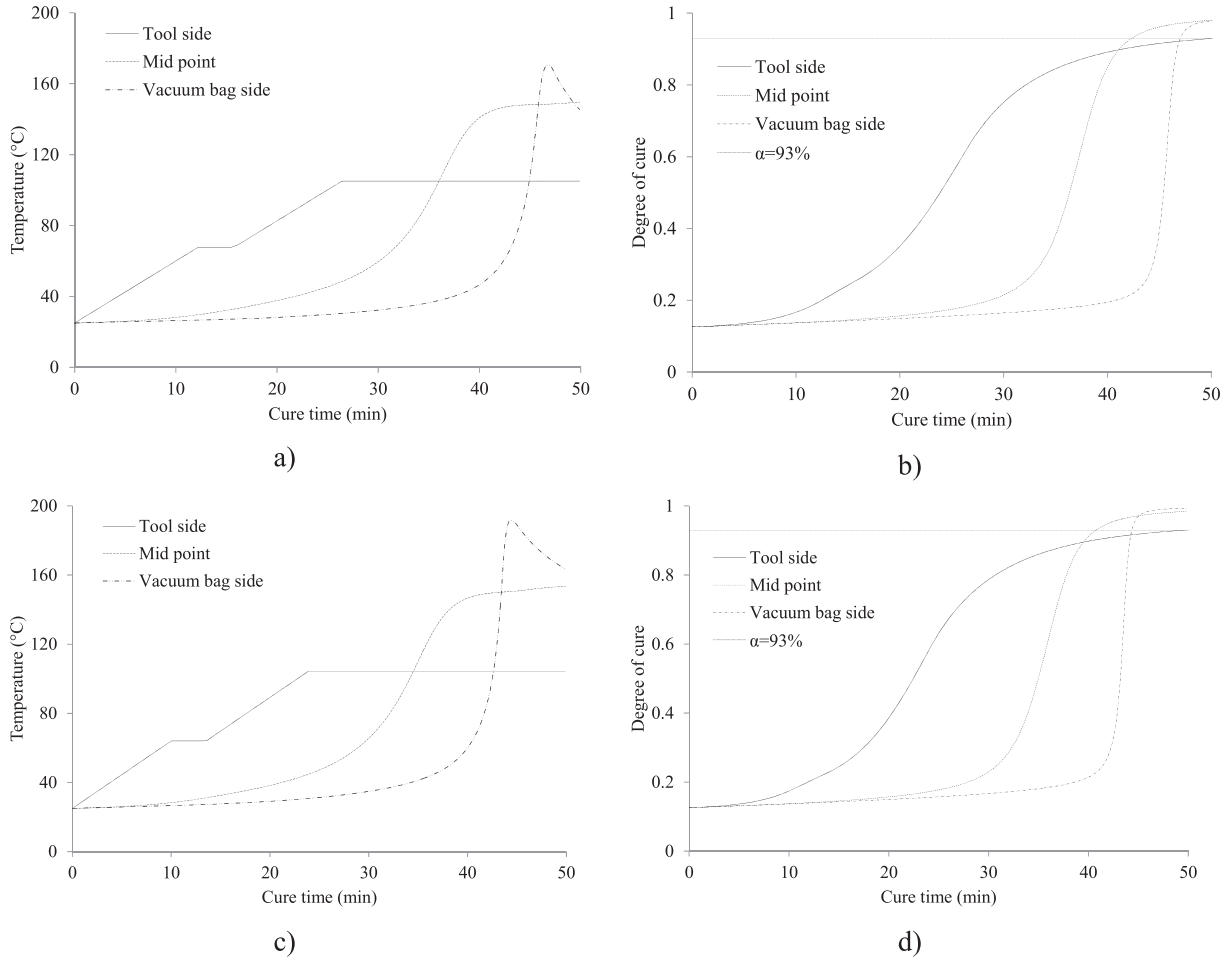

Fig. 9. Non-conservative solution details for the 50 mm flat panel: (a, b) individual C, (c, d) individual C'.

conservative zone. Optimal individuals (i.e. A′, B′, C′) showed to have a convection coefficient of about 1 W/m^2 °C meaning that the application of insulation is beneficial also for the 50 mm thick panel. However it is only in the case of conservative individuals (i.e. A′) that differences in cure profiles can be found whilst in the case of transitional and non-conservative individuals (i. e. B′, C′ respectively) the cure profile look similar to the case without convection coefficient as parameter. It is interesting to notice that in this case due to the larger thickness at play, individual A′ presents a first dwell temperature of about 42 °C which is 10 °C less than individual A. This is opposite behaviour compared to the 10 mm scenario suggesting that for thicker parts the effect of applying lower convection coefficients needs to be counteracted by a decrease in first dwell temperature and longer first dwell duration (i. e. 77 min for individual A′). To understand why there is a difference in the cure behaviour for A and C, the cure and temperature profiles of the 50 mm case will be investigated in more detail in Section 5.3.4.

5.3.3. Flat panel 100 mm results

Fig. 8 illustrates the optimisation results for the flat panel 100 mm cases. The convergence is reached after 11 generations and proved to be the most demanding optimisation problem with a computational time of 2820 min. The Pareto front seems to show a change in convexity, however this has to be attributed to the minimum temperature allowed in the optimisation (i.e 30 °C). Lower curing temperatures would result in the standard L-shaped Pareto, however these temperature are not possible in practice therefore are excluded in the first dwell temperature range. Analysis of the design parameters of the Pareto individuals allow to identify common trends within same clusters of individuals. Candidate individuals (i.e. A, B, C, A′, B′, C′) are selected and highlighted in Fig. 8 whilst the corresponding design parameters are reported in Table 5. All the individuals present second dwell in the range of 100–104 °C. When the convection coefficient is not used as parameter, the first dwell temperature is at its lowest compared to the 10 and 50 mm case. Individual A in the conservative zone has a first dwell temperature of about 30 °C, Individual B 40 °C and individual C 52 °C. The strategy for these points is dictated by the high thickness at play and makes the degree of cure develop at a low temperature to lower the chemical potential of the reaction when the ramp to the second dwell occurs. The first dwell duration for individual A and B are in the range of 80–90 min whilst the individual C has a short first dwell which brings the profile to the high second dwell temperature resulting in the shortest t_{cure}. The introduction of convection coefficient as optimisation parameter introduces benefits for the individual in the conservative and transitional zone (i.e. A′, B′). The optimal convection coefficient is in the range of 1–3.4 W/m^2 °C which means application of insulation at the bag side. In specific individuals A′ and B′ show shorter first dwell duration and higher second dwell temperature compared to individual A and B. Furthermore, non-conservative zone individuals in both 50 and 100 mm case (i. e. C, C′) are obtained essentially applying one dwell cure profile leading to a fast process but larger amount of process induced defects.

5.3.4. Effect of convection coefficient on Pareto fronts

From the observation of Figs. 6–8 and Table 5, it is possible to notice that the convection coefficient always tends towards insulation of the vacuum bag side which is in contrast to results shown in [4]. In that study, the effect of different convection coefficients on Pareto fronts has been investigated in the case of curing inside a fan oven. The results in

this case showed Pareto front worsened when a lower convection coefficient is applied. In that case, unlike the problem currently under study, the sink temperature of the convection boundary condition followed the cure profile since the cure process occurred in the oven. Therefore application of insulation in this case would trigger uncontrolled exothermic reaction leading to worse thermal gradients through thickness.

In the current study, the effect of convection coefficient is investigated when the curing occurs by means of hot tool plate for a single mould process. In this scenario the sink temperature of the convection boundary condition is equal to ambient temperature. Therefore, applying a lower convection coefficient at the vacuum bad side influenced the process positively shifting the Pareto towards shorter t_{cure} and lower $\Delta\alpha_{max}$. However the magnitude of the benefits brought differs. For the 10 mm case the benefits are similar throughout the different zones whilst for the 50 mm and 100 mm case only the conservative zone individuals see a significant benefit. In order to understand this behaviour it is necessary to look at the temperature and degree of cure evolution through thickness of individuals belonging to different zones. Fig. 9 illustrates the temperature and degree of cure evolution of the non-conservative points for the 50 mm flat panel in the case when convection coefficient is not used as optimisation parameter (a and b respectively) corresponding to point C in Fig. 7 and in the case when it is an optimisation parameter (c and d respectively) corresponding to point C′ in Fig. 7. The application of a convection coefficient equal to 1 W/m^2 °C (i.e. insulation) in this case does not generate different curing behaviours. The two solutions are equivalent and only the magnitude of the temperature overshoot generated at the vacuum side changes, being 10 °C higher for individual C′. In both cases, due to the exotherm generated, the last region to reach the target degree of cure is the one in contact with the tool. Fig. 10 presents the temperature and degree of cure evolution of the conservative points for the 50 mm flat panel in the case when convection coefficient is not used as optimisation parameter (a and b respectively) corresponding to point A in Fig. 7 and in the case when it is an optimisation parameter (c and d respectively) corresponding to point A′ in Fig. 7. In this case the benefits brought by the application of a convection coefficient equal to 1 W/m^2 °C (i.e. insulation) are significant, about 30% reduction in t_{cure} and about 65% in $\Delta\alpha_{max}$. It is possible to notice in the temperature evolution plots that when insulation is applied, the region at the vacuum bag side experiences a significant temperature overshoot. This reflects in a different cure evolution compared to the non-insulated case. From the degree of cure evolution it is possible to highlight that when the vacuum bag side of the flat panel experiences temperature overshoot, the last region to cure is the one touching the tool whilst when no temperature overshoot occurs it is the vacuum bag side that completes the cure last. This highlights that exothermic effect when controlled and understood can be very beneficial.

Fig. 11 reports the temperature and degree of cure evolution for the individual A of the 50 mm flat panel case. In one simulation, Fig. 11(a, b) a convection coefficient of 18 W/m^2 °C was applied whereas in the second simulation the convection coefficient was equal to 9 W/m^2 °C. The convection coefficients were chosen to be equally spaced from the standard convection coefficient (i.e. 13.6 W/m^2 °C). The simulations are intended to isolate the effect of convection coefficient on degree of cure evolution. The evolution of the degree of cure can be compared with Fig. 10(a, b) in which convection coefficient is 13.6 W/m^2 °C and the process ended with a $\Delta\alpha_{max}$ equal to 0.33. It can be noted that

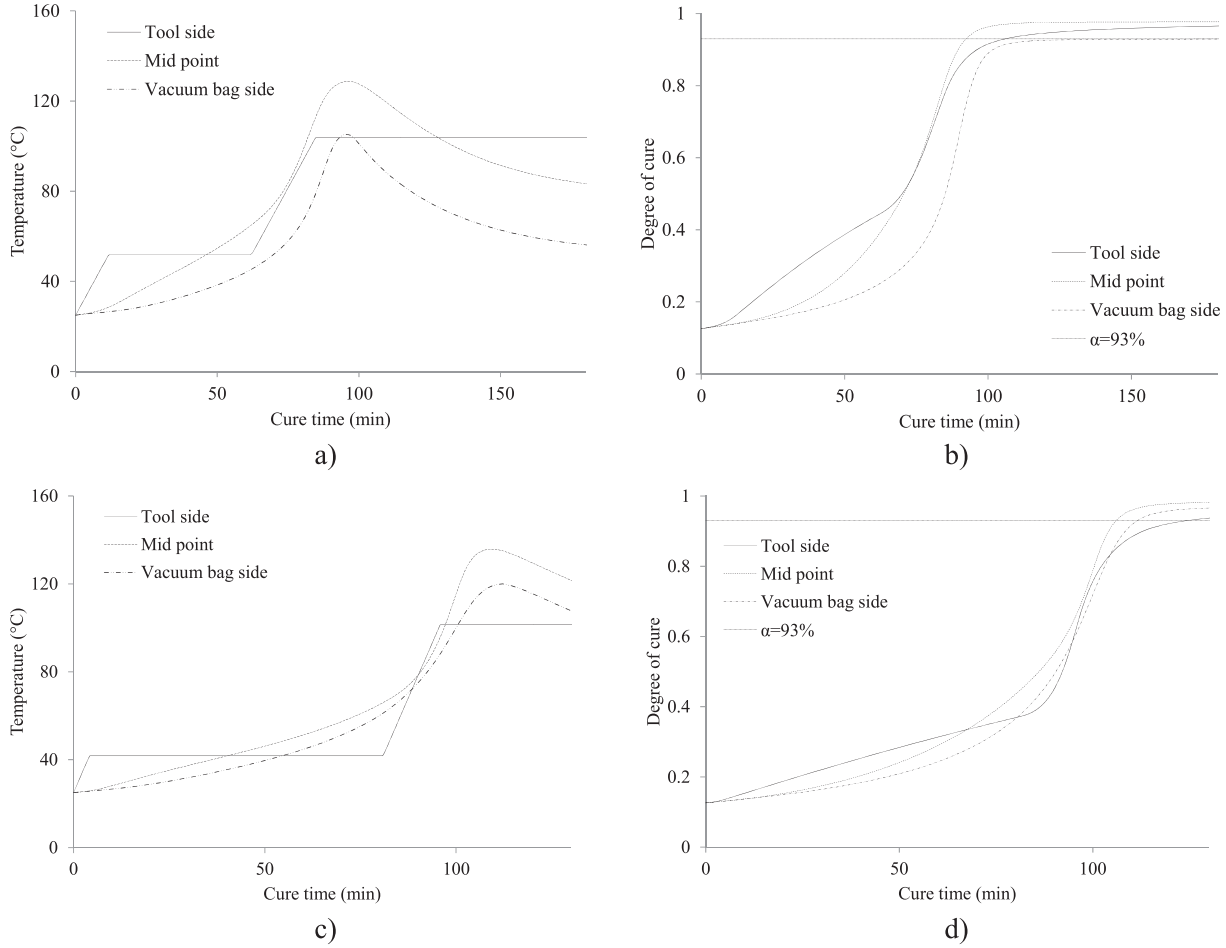

Fig. 10. Conservative solution details for the 50 mm flat panel: (a, b) individual A, (c, d) individual A′.

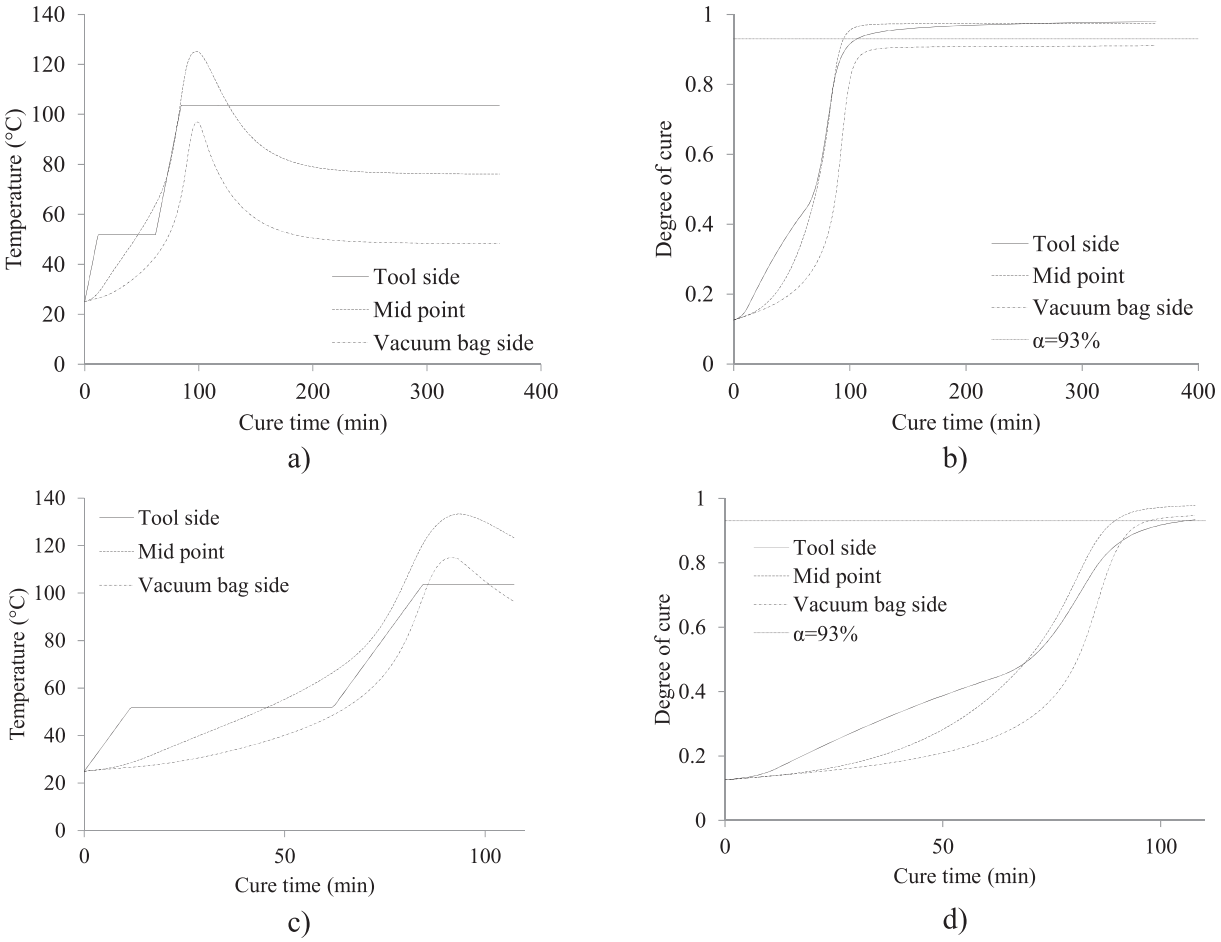

Fig. 11. Individual A solution details for the 50 mm flat panel: (a, b) h = 18 W/m^2 °C, (c, d) h = 9 W/m^2 °C.

increasing the convection coefficient (i.e. 18 W/m^2 °C) leads to a larger temperature gradient through thickness and consequently in degree of cure (i.e. 0.36) whilst a decrease in convection coefficient (i.e. 9 W/m^2 °C) leads to smaller temperature and degree of cure gradients (i.e. 0.26). Furthermore, it points out that the midpoint temperature is slightly affected by the change in convection coefficient and that is the vacuum bag side region to experience the biggest change in temperature due to the change in convection coefficient. This leads in the case of Fig. 11(a, b), to fail to reach the 93% minimum degree of cure target for the point at the vacuum bag side strengthening the significant role played by the convection coefficient in the process.

5.3.5. Effect of thickness on Pareto fronts

Fig. 12 depicts the comparison of the Pareto front for the three thicknesses when natural convection is applied at the bag side. All the individuals belonging to the non-conservative zone end up with a short first dwell duration (about 2 mins) making the cure profile a quasi-one dwell. The results show a clear influence of thickness on the Pareto front. A previous work showed that higher thicknesses leads to Pareto fronts shifted towards higher t_{cure} and maximum $\Delta\alpha_{max}$ for thicknesses in the range of 3–24 mm [41]. This holds for the 50 and 100 mm Pareto fronts. The 100 mm Pareto fronts is about 50 mins shifted towards longer t_{cure} and 0.03 towards higher $\Delta\alpha_{max}$. The Pareto front for 10 mm case does not fall within this framework. This can be explained considering that the cure behaviour of the 50 mm and 100 mm case are alike both involving temperature overshoots whilst the 10 mm case involves a cure evolution with no temperature overshoot occurrence hence a comparison with the other Pareto fronts is not meaningful in this case. Furthermore, the Pareto fronts for the 50 mm and 100 mm

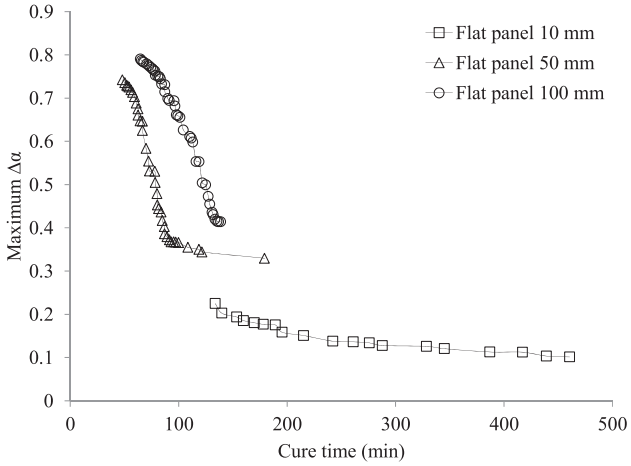

Fig. 12. Thickness' influence on Pareto front.

show the majority of their solutions in the non-conservative zone whereas the 10 mm Pareto front has the majority of the solutions in the conservative zone. This is related to the selection of parameters ranges and the nature of the resin of the study. The first dwell lowest temperature selected is 30 °C. The selection of first dwell temperature lower than 30 °C would probably fill the conservative zone of the Pareto fronts for the 50 mm and 100 mm case. However curing temperatures lower than 30 °C are not feasible in practice and therefore have not been considered in this study. On the other hand the selection of temperature ranges proves to be very conservative in the case of 10 mm. This

Table 6
MRCC application results.

Thickness	T_i (°C)	Δt (min)	r (°C min^{-1})	α_{max}	t_{cure} (min)
Thin (10 mm)	70	240	0.33	88%	370
Thick (50 mm)	70	240	0.33	87%	370
Ultra-thick (100 mm)	70	240	0.33	93%	370

highlights the importance of appropriate selection of design parameters and the necessity of optimisation methodology at the design stage.

5.3.6. Comparison with MRCC solutions

Table 6 reports the results obtained when MRCC has been applied to the different thicknesses cases**.** The MRCC fails to reach the 93% degree of cure requirement for both the 10 mm and 50 mm case stopping at 88% and 87% respectively. It is not meaningful therefore to quantify the benefits introduced by optimal solutions in terms of t_{cure} and $\Delta\alpha_{max}$ reduction since the process as a matter of fact failed to meet the quality requirements when MRCC was applied. With regards to the 10 mm and 50 mm cases the exothermic reaction generated by the MRCC is not strong enough to overcome the cool down due to the convection on the vacuum bag side; as a consequence the top part experience a colder thermal history that is not sufficient to reach the 93% requirement. For the 100 mm case the MRCC generated a solution meeting the set degree of cure requirements ending in 370 min and with a $\Delta\alpha_{max}$ equal to 0.56. When compared to the solution obtained with the MRCC, the selection of Pareto points belonging to the conservative zone could lead up to 60% t_{cure} reduction and up to 30% $\Delta\alpha_{max}$ reduction. Any point in the Pareto brings t_{cure} reduction greater than 60% therefore an engineering choice could be to maximise the reduction in $\Delta\alpha_{max}$ hence selecting individuals in the conservative zone.

6. Conclusions

In the present paper the chemical characterisation involving cure kinetics and Di Benedetto equation of the two components system Airstone 780E epoxy resin and 785H Hardener has been successfully undertaken. The relevant material models have been built. A heat transfer model considering heat generation from the cure process has been developed, implemented and validated through test. The cure simulation implemented in the FE solver Marc.Mentat constitutes the first published work describing the cure evolution of the system under study.

The multi-objective optimisation methodology developed is able to identify efficient design points for the manufacturing of thin, thick and ultra-thick components for the wind turbine industry, represented by 10, 50 and 100 mm in this study. However the results can be extended also to other fields. The multi-objective set-up optimises the two objectives (cure time: t_{cure} and quality: $\Delta\alpha_{max}$) independently without the need to assume a priori the weights/benefits associated to each objective. The final Pareto fronts contain solutions with different prioritisation of the objectives each one would be the solution of a specific weighted fitness function. The Pareto fronts show the competitive nature of two objectives selected. The multiple optimal design points in the Pareto can be ranked and selected according to the quality/cost ratio required by the end user. The results highlight that MRCC generates parts with lower final degree of cure and results in unnecessary long cure times. In the case of the 100 mm thick flat panel t_{cure} reduction up to 60% and $\Delta\alpha_{max}$ reduction up to 30% can be achieved compared to the solution obtained with MRCC. Moreover, an investigation of the influence of thicknesses on Pareto fronts demonstrated that higher thicknesses shift the efficient solutions towards higher $\Delta\alpha_{max}$ level and longer t_{cure} unveiling the hidden relationship between thickness and minimum Pareto front achievable.

Furthermore, the study suggests the idea of using convection coefficient as a new design parameter to consider alongside thermal profile. Introduction of the convection coefficient as additional parameter in the optimisation showed that the convection coefficient tends towards insulation values for all points studied ($< 13.6\ W/m^2\ °C$). The application of insulation at the vacuum bag side can lead to significant improvement in both t_{cure} and $\Delta\alpha_{max}$ reduction especially for points belonging to the conservative zone of the Pareto fronts. This could be achieved in first instance by placing insulating blankets at the vacuum bag side to decrease the heat exchange with the environment. Different thicknesses for the insulating material would generate different levels of insulation. Characterisation of the aforementioned blankets would be required before its use in industrial application. The measurement technique adopted in [38] can be implemented for this purpose. The same study shows that the measurements of convection coefficient shows local variability therefore challenges are foreseen with regard to this type of characterisation. Detailed analysis of the temperature and degree of cure evolution of individuals belonging to two different zones in the Pareto front of the 50 mm thick flat panel proved that the insulation is particularly beneficial when it introduces changes in the cure mechanisms by triggering exothermic phenomena through the thickness intense enough to allow the vacuum bag side to cure faster than tool side. A further benefit of about 30% reduction in t_{cure} and 65% reduction in $\Delta\alpha_{max}$ compared to optimal solutions obtained when natural convection coefficient was applied at the bag side can be achieved. It has to be noted that the strategy selected contributes to a uniformity of the cure through thickness which reflects into higher mechanical performances. The findings of the paper pointed out that exothermic effect can be used to improve the quality and efficiency of the manufacturing process when predicted and controlled and that appropriate insulation can help achieving it. More than this, the methodology implemented is an important step forward towards a first time right design of the process which can reduce scrapped parts and waste material, improve the quality of the final part, reducing cost and facilitating scheduling.

Further investigations require definition of stability areas and robustness of the solutions in the Pareto fronts. Considerations regarding deviations from nominal values for boundary and initial conditions are necessary. Discarding optimal solutions that presents high level of variability will lead to the generation of more robust Pareto fronts hence robust design choices.

Acknowledgments

This work was supported by ADEM innovation lab, A green Deal in Energy Materials of the Ministry of Economic Affairs of the Netherlands (www.adem-innovationlab.nl). Data underlying this research are available through the repository of the Dutch Universities of Technology, http://researchdata.4tu.nl/home, with https://doi.org/10.4121/uuid:59c4e711-2003-48ff-ae22-e936e017f418.

References

[1] Antonucci V, Giordano M, Hsiao K-T, Advani SG. A methodology to reduce thermal gradients due to the exothermic reactions in composites processing. Int J Heat Mass Transfer 2002;45(8):1675–84.
[2] Bogetti TA, Gillespie JW. Process-induced stress and deformation in thick-section thermoset composite laminates. J Compos Mater 1992;26(5):626–60.
[3] Sorrentino L, Polini W, Bellini C. To design the cure process of thick composite parts: experimental and numerical results. Adv Compos Mater 2014;23(3):225–38.
[4] Struzziero G, Skordos AA. Multi-objective optimisation of the cure of thick components. Compos A Appl Sci Manuf 2017;93:126–36.
[5] Li M, Tucker III CL. Optimal curing for thermoset matrix composites: thermochemical and consolidation considerations. Polym Compos 2002;23(5):739–57.
[6] Li M, Zhu Q, Geubelle PH, Tucker III CL. Optimal curing for thermoset matrix composites: thermochemical considerations. Polym Compos 2001;22(1):118–31.
[7] Pagano RL, Calado VMA, Bezerra de Souza M, Biscaia EC. Proposal of an optimum cure cycle for filament winding process using a hybrid neural network - first principles model. Polym Compos 2014;35(7):1377–87.

[8] Pillai VK, Beris AN, Dhurjati PS. Heuristics guided optimization of a batch autoclave curing process. Comput Chem Eng 1996;20(3):275–94.
[9] Pillai V, Beris AN, Dhurjati P. Intelligent curing of thick composites using a knowledge-based system. J Compos Mater 1997;31(1):22–51.
[10] Pillai VK, Beris AN, Dhurjati PS. Implementation of model-based optimal temperature profiles for autoclave curing of composites using a knowledge-based system. Ind Eng Chem Res 1994;33(10):2443–52.
[11] Rai N, Pitchumani R. Optimal cure cycles for the fabrication of thermosetting-matrix composites. Polym Compos 1997;18(4):566–81.
[12] Skordos AA, Partridge IK. Inverse heat transfer for optimization and on-line thermal properties estimation in composites curing. Inverse Prob Sci Eng 2004;12(2):157–72.
[13] Yang ZL, Lee S. Optimized curing of thick section composite laminates. Mater Manuf Process 2001;16(4):541–60.
[14] Aleksendrić D, Carlone P, Ćirović V. Optimization of the temperature-time curve for the curing process of thermoset matrix composites. Appl Compos Mater 2016;23(5):1047–63.
[15] Bailleul JL, Sobotka V, Delaunay D, Jarny Y. Inverse algorithm for optimal processing of composite materials. Compos A Appl Sci Manuf 2003;34(8):695–708.
[16] Gopal AK, Adali S, Verijenko VE. Optimal temperature profiles for minimum residual stress in the cure process of polymer composites. Compos Struct 2000;48(1):99–106.
[17] Jahromi PE, Shojaei A, Reza Pishvaie SM. Prediction and optimization of cure cycle of thick fiber-reinforced composite parts using dynamic artificial neural networks. J Reinf Plast Compos 2012;31(18):1201–15.
[18] Kam TY, Lai FM, Sher HF. Optimal paramerers for curing graphite/epoxy composite laminates. J Mater Process Tech 1995;48(1–4):357–63.
[19] Kennedy GJ, Hansen JS. The hybrid-adjoint method: a semi-analytic gradient evaluation technique applied to composite cure cycle optimization. Optim Eng 2010;11(1):23–43.
[20] Olivier P, Cottu JP. Optimisation of the co-curing of two different composites with the aim of minimising residual curing stress levels. Compos Sci Technol 1998;58(5):645–51.
[21] White SR, Hahn HT. Cure cycle optimization for the reduction of processing-induced residual stresses in composite materials. J Compos Mater 1993;27(14):1352–78.
[22] Zhu Q, Geubelle PH. Dimensional accuracy of thermoset composites: Shape optimization. J Compos Mater 2002;36(6):647–72.
[23] Michaud DJ, Beris AN, Dhurjati PS. Thick-sectioned RTM composite manufacturing, Part II. Robust cure cycle optimization and control. J Compos Mater 2002;36(10):1201–32.
[24] Pantelelis N, Vrouvakis T, Spentzas K. Cure cycle design for composite materials using computer simulation and optimisation tools. Forschung Ingen/Eng Res 2002;67(6):254–62.
[25] Pantelelis NG. Optimised cure cycles for resin transfer moulding. Compos Sci Technol 2003;63(2):249–64.
[26] Ruiz E, Trochu F. Comprehensive thermal optimization of liquid composite molding to reduce cycle time and processing stresses. Polym Compos 2005;26(2):209–30.
[27] Ruiz E, Trochu F. Multi-criteria thermal optimization in liquid composite molding to reduce processing stresses and cycle time. Compos A Appl Sci Manuf 2006;37(6 SPEC. ISS):913–24.
[28] Vafayan M, Ghoreishy MHR, Abedini H, Beheshty MH. Development of an optimized thermal cure cycle for a complex-shape composite part using a coupled finite element/genetic algorithm technique. Iran Polym J (English Ed) 2015;24(6):459–69.
[29] Tifkitsis KI, Mesogitis TS, Struzziero G, Skordos AA. Stochastic multi-objective optimisation of the cure process of thick laminates. Compos A Appl Sci Manuf 2018;112:383–94.
[30] Airstone™ Infusion System Product. < www.dowepoxysystems.com > .
[31] Shi L. Heat transfer in the thick thermoset composites; 2016.
[32] Struzziero G, Remy B, Skordos AA. Measurement of thermal conductivity of epoxy resins during cure. J Appl Polym Sci 2018;136(5):47015.
[33] Skordos AA. Modeling and monitoring of resin transfer moulding; 2000.
[34] Farmer JD, Covert EE. Thermal conductivity of a thermosetting advanced composite during its cure. J Thermophys Heat Transfer 1996;10(3):467–75.
[35] Marc® volume A: theory and user information; 2015. < www.mscsoftware.com > .
[36] Marc® volume B: element library; 2015. < www.mscsoftware.com > .
[37] Marc® volume D: user subroutines and special routines; 2015. < www.mscsoftware.com > .
[38] Mesogitis TS, Skordos AA, Long AC. Stochastic heat transfer simulation of the cure of advanced composites. J Compos Mater 2015;50(21):2971–86.
[39] Khoun L, Centea T, Hubert P. characterization methodology of thermoset resins for the processing of composite materials — case study: cycom 890rtm epoxy resin. J Compos Mater 2010;44(11):1397–415.
[40] Pascault JP, Williams RJJ. Relationships between glass transition temperature and conversion. Polym Bull 1990;24(1):115–21.
[41] Struzziero G, Skordos AA. Multi-objective optimisation of composites cure using genetic algorithms. In: ECCM15 – 15th european conference on composite materials. Venice, Italy; 2012.